

Radon-222 budget in Catalina Harbor, California: 1. Water mixing rates

S. L. Colbert,¹ D. E. Hammond and W. M. Berelson

Department of Earth Science, University of Southern California, Los Angeles, California 90089-0740

Abstract

We describe mixing on the basis of the radon distribution in Catalina Harbor, a small embayment on the southwest side of Catalina Island, California. During June 1998, there was a 2–3-m-thick warm surface layer in the inner harbor, underlain by cooler water. A radon budget for this system was constructed with the objective of evaluating boundary fluxes and developing a box model to describe mixing and transport into and within the harbor waters. Benthic inputs were evaluated with in situ benthic flux chambers. Loss via decay and gas evasion was characterized by surveys of radon concentration in the water column. Closure of the budget required another large radon source, which was assumed to be tidal pumping of seawater through beach sands. The budget indicates that inputs were primarily attributable to benthic input (55%) and tidal pumping (38%). Losses were due to evasion to the atmosphere (29%), radioactive decay (35%), and mixing to the open ocean (36%). The average upwelling velocity into surface water was 0.73 m d^{-1} . Horizontal mixing was parameterized as an eddy diffusion, calculated to be $0.54 \pm 0.19 \text{ m}^2 \text{ s}^{-1}$, which was consistent with mixing predictions on the basis of scaling arguments.

The flushing of small harbors is often of concern, as their waters can be receptacles for waste discharged by boats and other activities. Catalina Harbor, California, is of interest because concerns have arisen about the potential effect of discharges from private boats and several fish stock pens that are currently in use for raising sea bass to stock West Coast fisheries. Sound management policies need to be based on a firm understanding of the sources and fates of nutrients and pollution within the harbor and require knowledge of the mixing regime.

Water column mixing between coastal embayments and harbors with limited communication with open ocean waters are dominated by complicated local effects such as shallow bathymetry, winds, and tides. Physical models of water mixing in harbors require extensive data sets, expensive current meters for ground truthing, and extensive computer processing capabilities. In addition, these models can only predict the bulk transport of water. The transport of dissolved matter, such as nutrients and pollutants, will depend on rates of dispersion that cannot be obtained from a physical mixing model. To obtain these rates, studies that apply a tracer, such as ^{222}Rn (radon), are needed.

¹To whom correspondence should be addressed. Present address: Department of Geology, University of Puget Sound, Tacoma, Washington 98416 (scolbert@alumni.usc.edu).

Acknowledgments

We thank Tony Michaels, Liz Capporelli, Kevin Flanagan, Julian Herndon, and Doug Conlin, who made the fieldwork possible. Hongyu Huang, Jason Masters, and Reni Schimmoeller helped with the fieldwork. We also thank two anonymous reviewers for their useful comments.

This study would not have taken place without the financial and logistical support of the Wrigley Institute for Environmental Studies and Catalina Marine Science Center. This research was conducted with support from the University of Southern California Sea Grant Program, part of the National Sea Grant College Program, National Oceanic and Atmospheric Administration, U.S. Department of Commerce, under grants NA86RG0054 and NA16RG2256.

Radon is a naturally occurring radioisotope that is an intermediate in the ^{238}U decay series. It has a 3.8-d half-life and is formed by decay of its long-lived radium parent, ^{226}Ra (1,600-yr half-life). Radium is an element of relatively low solubility and is concentrated in or on the surfaces of solids, although some radium is dissolved in seawater. As a result, sediments are a strong source of radon. Radon is a noble gas and behaves conservatively in the sediments. Radon can be used as a tracer for the exchange of dissolved substances across the sediment–water interface (Broecker 1965). As radon is produced, it migrates by molecular diffusion from its source and is also transported by irrigation of burrows by infauna (Hammond and Fuller 1979), fresh groundwater flow (Cable et al. 1996), and physical flow through sediments driven by wave motion or tidal pumping as sea level rises and falls (Colbert et al. 2008). These processes generate radon concentration gradients above the seafloor that can be used to compute vertical mixing rates (Broecker et al. 1968; Berelson et al. 1982). When water containing radon is exposed to the atmosphere, radon can exchange across the interface, and in favorable settings it can be used as a tracer to estimate the exchange rate of dissolved gases across the air–water interface (Broecker and Peng 1971; Smethie et al. 1985).

In this paper, the radon distribution and thermal structure of a small, natural harbor are presented. Then, two different methods are applied to measure the benthic flux of radon to the water column. With these data, a mass balance computed for the head of the harbor reveals that an additional source of radon, presumably tidal pumping of seawater through beach sands, is required to balance the budget. Finally, a multibox model for Catalina Harbor is constructed to compute the upwelling and horizontal mixing rates.

Study site

Catalina Harbor is a small harbor located on the southwest side of Santa Catalina Island, California, about

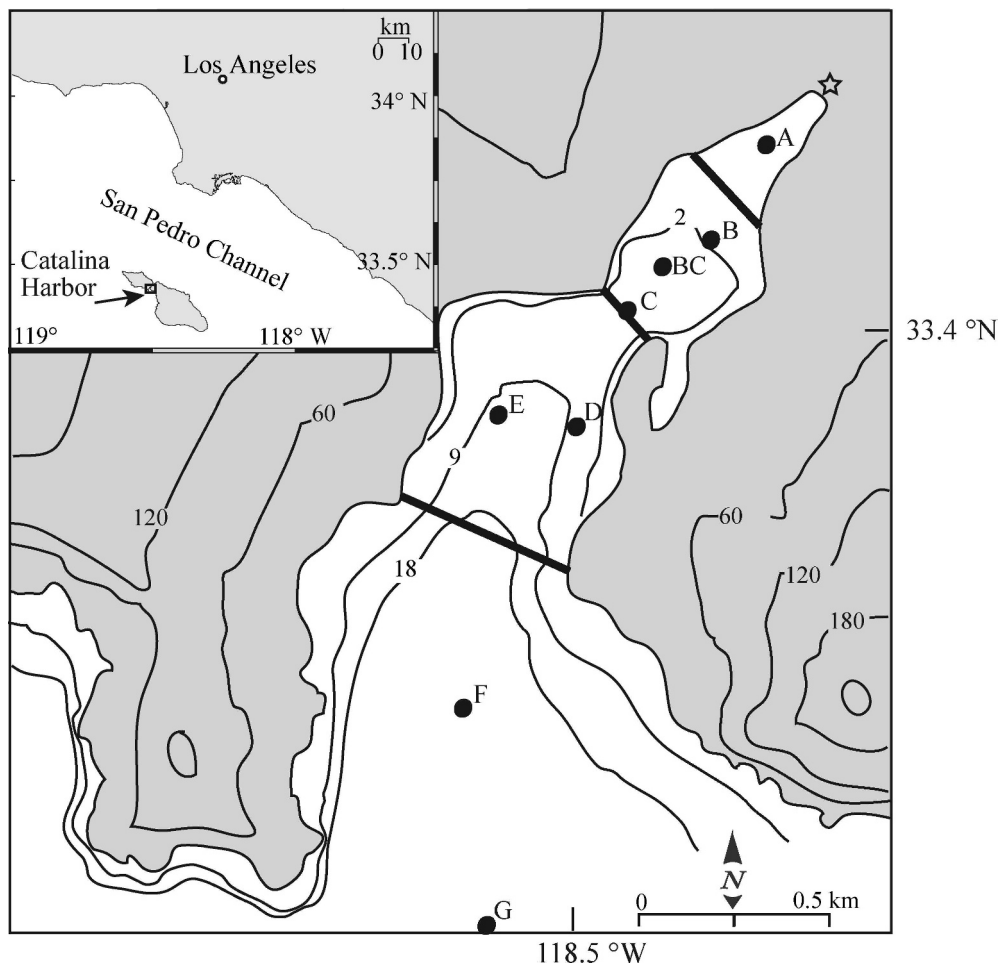


Fig. 1. Map of Catalina Harbor, California. Eight lettered stations that were occupied during this experiment are shown. Solid lines across the harbor demarcate boxes used for the radon mass balance. The star at the head of the harbor identifies the location of the tidal pumping experiment discussed in an accompanying paper (Colbert et al. 2008). Inset shows a regional map of Los Angeles, California, and Santa Catalina Island.

35 km southwest of Los Angeles (Fig. 1). At the head of the harbor is the narrowest part of the island, approximately 1 km wide, where the small town of Two Harbors caters to sailors arriving at either side of the isthmus. The axis of the harbor is oriented northeast-southwest, and the harbor is surrounded by topographic highs on either side that provide some shelter from the wind. The bathymetry along these sides drops off quickly, and the shoreline is primarily rocky with some sandy areas. At the head of the harbor, the bathymetry shoals to a broad, shallow (<2 m) region that is surrounded by a sandy beach and a gentle plain. During the study period, tides were mixed and had an average range of 1.1 m.

The shallow parts of the harbor range from sandy to rocky. In areas deeper than 3–4 m, sediments become silty sands and were often covered with a veneer of silts, which were easily resuspended and make it difficult for divers to observe the bottom. Despite the limited visibility, holes in the sediment surface suggest the presence of benthic fauna.

The climate is Mediterranean, with mild temperatures buffered by the cool seawater. The weather during the

study was typical for the summer months: fog at night that burns off in the morning, with steady winds blowing toward the head of the harbor throughout the afternoon. There are no surface freshwater sources to the harbor during the dry summer months.

Methods

Hydrographic study—A series of stations were defined within the harbor (Table 1), with closer station spacing at the head of the harbor where the bathymetry changes rapidly (Fig. 1). The water depth at the stations ranged from 0.9 m to 67 m. Several surveys of dissolved oxygen, temperature, and salinity were taken using hand-held probes (Yellow Springs Instruments) to try to define the hydrographic characteristics. The accuracy of the probes was $\pm 0.1^\circ\text{C}$ for temperature, ± 0.1 for salinity, and $\pm 5\%$ for oxygen.

Radon analysis—For water column samples, about 20 liters of water were collected by drawing water into

Table 1. Water depth and distance from the head of Catalina Harbor for each station.

Sta. ID	Distance (m)	Depth (m)
A	210	0.9
B	400	1.6
BC	560	6.0
C	650	7.7
D	870	7.3
E	920	9.6
F	1,530	39.3
G	2,010	66.7

evacuated bottles. Surface water samples were collected by lowering a hose to about 0.5 m depth; deeper waters were collected by using a small pump to draw water from depth and take a split of the flow into a radon bottle. No bubbles were observed in the flow lines during sampling. These samples were analyzed following the procedure outlined by Mathieu et al. (1988). All radon concentrations were calculated after accounting for decay that occurred between sample collection and when it was analyzed.

Sediment core—One sediment push core was collected by a diver near Sta. B in 3 m of water. Numerous small burrows could be seen in the upper few centimeters, with small worms crawling about. At 10- to 15-cm depth, the core appeared to have a cavity that could be a burrow, but it was not clear whether it was in communication with the overlying water. Upon returning to the laboratory, the core was sectioned and the muds were placed in incubation jars. The muds were analyzed for radon, stored for 5 d, and reanalyzed to measure the radon emanation rate. Splits of the mud were also collected and weighed to assess the porosity of each section.

Radon emanation analysis—The sediment radon emanation rate (E) was measured using a slurry technique (Hammond and Fuller 1979; Key et al. 1979; Mathieu et al. 1988). Similarly, radon production in the water column was assessed by stripping the radon out of 20 liters of water, and allowing the radon to grow back into equilibrium. The radon emanation from solids was calculated after accounting for disequilibrium between radon ingrowth and secular equilibrium. For each sample, emanation measurements were repeated until the standard deviation in this parameter was less than 5%. The slurry technique has been shown to overestimate the radon emanation rate by 10% to 20% (Key et al. 1979; Smethie et al. 1981), and has been attributed to differences in porosity between the slurry and in situ (Hammond and Fuller 1979). For sands, the slurry does not significantly alter the porosity relative to in situ conditions, so the slurry effect was assumed to be negligible.

Diffusive sediment radon flux—The equilibrium radon concentration was calculated as $\lambda C_{\infty} = (1 - \phi)\rho E$, where λ is the radon decay constant ($1.26 \times 10^{-4} \text{ min}^{-1}$), ϕ is the porosity, and ρ is the sediment density, assumed to be

2.6 g cm^{-3} . The diffusive flux from the sediments was estimated as:

$$J_{\text{diff}} = \frac{(\lambda C_{\infty} - \lambda C_0)}{\lambda} \sqrt{\frac{D}{\lambda}} \quad (1)$$

where λC_{∞} and λC_0 are, respectively, the equilibrium and interface radon activity concentrations in bulk sediment. The effective diffusivity, D , was computed by taking the molecular diffusivity at 18°C and salinity of 34 (Jähne et al. 1987) and adjusting for tortuosity as ϕ^2 (Ullman and Aller 1982). A porosity of 0.66 for the top interval indicates $D = 4.6 \times 10^{-6} \text{ cm}^2 \text{ s}^{-1}$.

Benthic flux chambers—Five benthic flux chambers were deployed by divers for 1-d periods to measure the radon flux. Flux chamber deployments followed the methods outlined by Berelson (1986). Flux chambers had a footprint of 730 cm^2 , and were continuously mixed with a rotating paddle. Chambers were sampled with two 140-mL syringes at the beginning and end of each deployment. Water from the first syringe was filtered (60 mL through $0.4 \mu\text{m}$) and the remainder was transferred with minimal gas contact into a syringe barrel with no plunger (filling from the bottom). An oxygen probe was inserted and oxygen concentration relative to saturated surface water was measured. Initial oxygen concentrations were assumed to be near saturation, and oxygen fluxes were calculated by:

$$J_{\text{O}_2} = \frac{([O_2]_t - [O_2]_i)h}{t} \quad (2)$$

where subscripts t and i denote the final and initial oxygen concentration ($\mu\text{mol L}^{-1}$), h is the chamber height (m), and t is the deployment time (s). The water in the second syringe was used to slowly fill a glass bulb, with minimal contact with air. This sample was subsequently analyzed with the rapid radon extraction system (Berelson et al. 1987). Radon fluxes were calculated as:

$$J_{\text{sed}} = \frac{h}{60} \left\{ \frac{(\lambda C_t - \lambda C_i) \exp(-\lambda t)}{1 - \exp(-\lambda t)} - P \right\} \quad (3)$$

J_{sed} is the radon flux in units of $\text{atoms s}^{-1} \text{ m}^{-2}$, λC is radon activity concentration (dpm m^{-3}) with subscripts i and t noting initial and final concentrations, respectively, P is dissolved ^{226}Ra activity concentration (disintegrations per minute [dpm m^{-3}]), which is further defined below, and the factor 60 is a unit conversion (min s^{-1}).

Observations

Stratification—Several surveys of dissolved oxygen, temperature, and salinity were taken in Catalina Harbor to try to define the hydrographic characteristics. Dissolved oxygen was within 10% of saturation at all sites studied. Salinity was only measured on the final day of field observations (16 June 1998) and in many of the discrete radon samples. These results showed uniform values within the resolution of the salinometer. Temperature showed a few degrees of variation, ranging from a maximum of

20.0°C near the head of the Harbor to 15.8°C at 20 m depth at Sta. G. There appears to be a persistent layer of warmer water 2 to 3 m thick that sits in the shoal area at the head of the harbor and mixes or flows horizontally seaward, toward the open ocean (Fig. 2). It also appears that cooler waters upwell a bit, as isotherms consistently rose slightly near the head of the harbor.

Water column radon—Radon was measured at each station, with vertical profiles made at the deeper stations (Table 2). Repeated sampling over the week of fieldwork showed that radon distributions at stations removed from large concentration gradients had less than 20% variation. Plotting the average concentration at each depth, we have assumed that the cross-section shown in Fig. 3 represents an average, steady-state distribution. Although the sampling density was much smaller, the radon distribution has similarities to the temperature field, with highest concentrations in the shallow water indicating a strong local source, and removal of radon due to gas exchange, horizontal mixing, and radioactive decay as it migrates toward the open ocean. At the seaward end (Sta. G), the first sampling period showed an anomalously high concentration with a corresponding warm temperature, but the source of this radon is unidentified. Presumably it reflected a transient outflow from another cove.

In situ benthic fluxes—Benthic flux chambers were deployed at two stations. Calculated fluxes for both oxygen and radon are given in Table 3. Attempts were also made to use these chambers to quantify advective flow through these sediments. Two of the three chambers (Blues and Rock) were designed to be seep meters, with a flexible water-filled bag that would deform if water flowed into (or out of) a sealed chamber. Changes in bag volume observed were +70 and -70 mL in each chamber during a 1-d deployment near Sta. B, so no significant fresh groundwater flow was observed. The third chamber (Jazz) had a small conduit to allow inflow or escape of water from the chamber during deployment; during the first deployment near Sta. B, there was some indication of elevated radon in a glass tube attached to the outlet, suggesting the possibility of outflow from the chamber. A redeployment of this chamber in 1 m depth near Sta. A showed elevated radon, again suggesting outflow from the chamber. Salinity in the chamber was also slightly elevated, consistent with a discharge of water from the beach, which had higher salinities (Colbert et al. 2008). Additional experiments with this type of seepage chamber deployed in shallow water produced inconsistent results (Berelson unpubl. data).

Diffusive flux—The radon emanation of solids was measured in one sediment core collected at Sta. B (Table 4). The decrease in radon emanation with depth was undoubtedly due to the presence of finer-grained sediments near the core top. Using these data, the diffusive radon flux from sediments was $27 \text{ atoms m}^{-2} \text{ s}^{-1}$. This is less than half of the observed in situ fluxes and indicates that significant

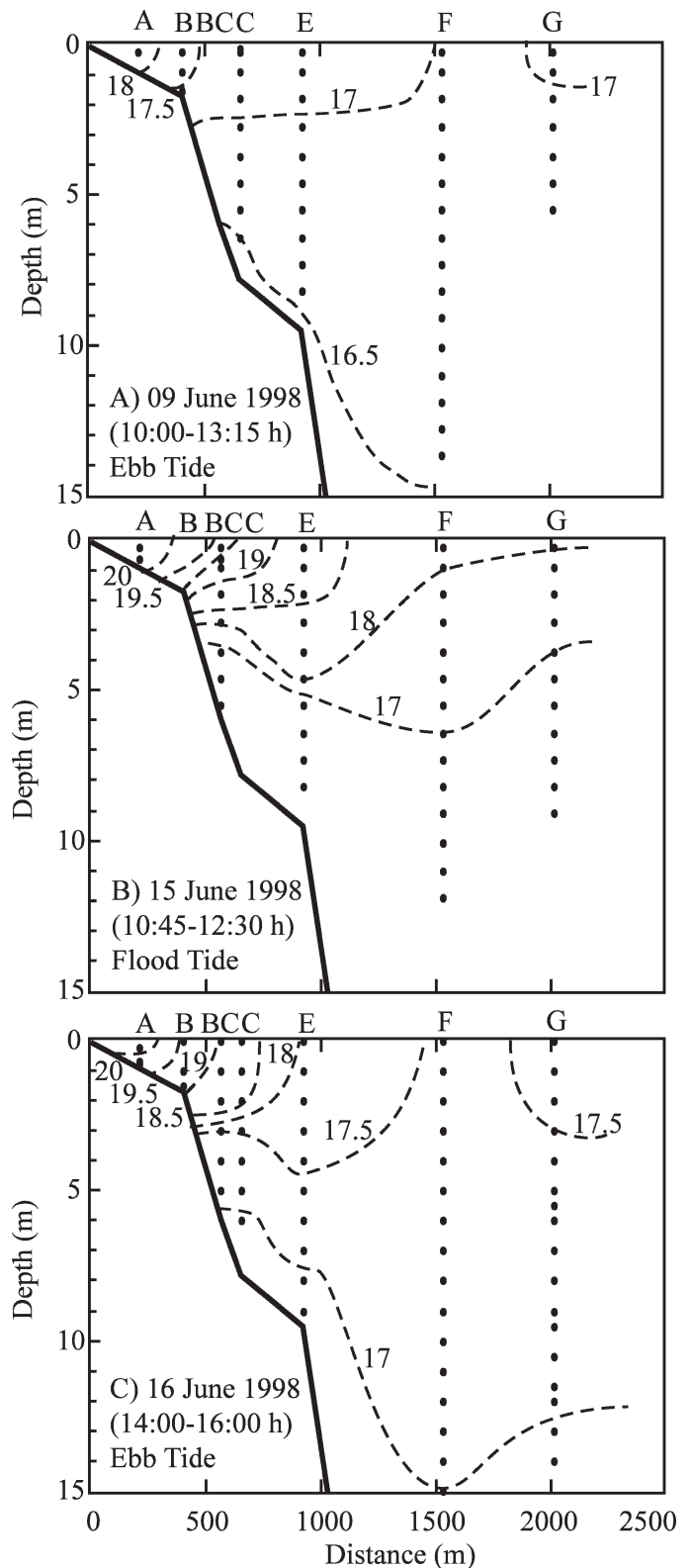


Fig. 2. Temperature profiles in a cross-section of the harbor on 3 d: (A) 09 June 1998, (B) 15 June 1998, and (C) 16 June 1998. Solid line is the seafloor, interpolated between stations. Circles represent individual measurements, and dashed lines are hand-drawn isotherms in °C.

Table 2. Radon data at each station. Measurement uncertainties are 1 SD on the basis of the counting statistics.

Sta. ID	Date and time collected	Depth (m)	Radon conc. (dpm L ⁻¹)
A	09 Jun 98 09:50 h	0.5	1.90±0.07
A	15 Jun 98 12:35 h	0.5	1.66±0.07
B	09 Jun 98 10:00 h	0.5	1.06±0.04
B	11 Jun 98 11:40 h	3.0	0.71±0.03
BC	10 Jun 98 15:03 h	0.5	1.39±0.05
BC	15 Jun 98 12:15 h	0.5	1.08±0.04
BC	15 Jun 98 12:28 h	5.5	0.31±0.02
BC	10 Jun 98 15:10 h	6.0	0.71±0.03
C	09 Jun 98 10:22 h	0.5	0.87±0.03
C	09 Jun 98 10:47 h	7.6	0.28±0.01
D	09 Jun 98 11:28 h	0.5	0.38±0.02
E	09 Jun 98 11:42 h	0.5	0.69±0.03
E	10 Jun 98 14:30 h	0.5	0.47±0.02
E	15 Jun 98 12:00 h	0.5	0.50±0.02
E	09 Jun 98 12:03 h	4.0	0.19±0.01
E	10 Jun 98 14:50 h	4.0	0.41±0.02
E	15 Jun 98 11:50 h	4.5	0.36±0.02
E	09 Jun 98 12:18 h	8.5	0.38±0.02
F	09 Jun 98 12:40 h	0.5	0.14±0.01
F	15 Jun 98 11:15 h	0.5	0.09±0.01
F	09 Jun 98 12:52 h	5.0	0.12±0.01
F	15 Jun 98 11:25 h	8.0	0.17±0.01
F	09 Jun 98 13:01 h	10.0	0.16±0.01
G	09 Jun 98 13:17 h	0.5	1.12±0.04
G	15 Jun 98 10:44 h	0.5	0.14±0.01
G	15 Jun 98 10:46 h	Air	0.078±0.006
San Pedro Channel	12 Jun 98 13:00 h	Air	0.059±0.004

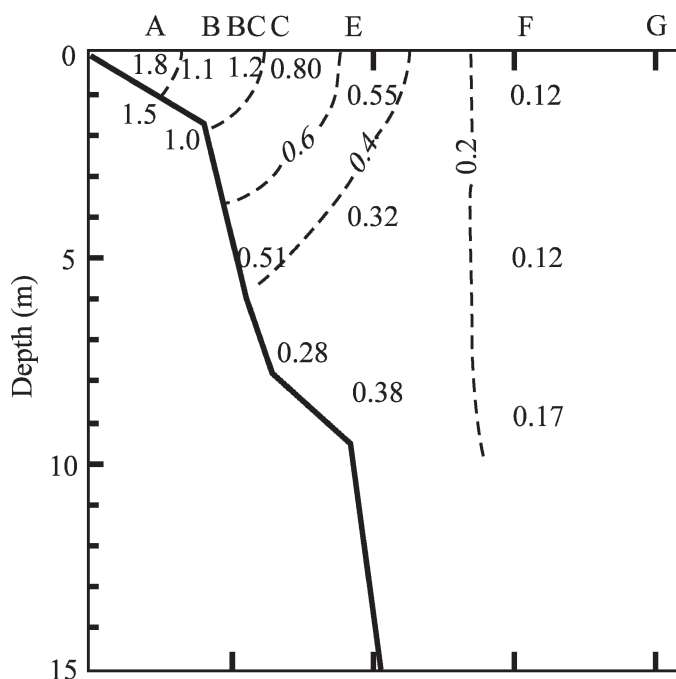


Fig. 3. Average radon distribution in a cross-section down the axis of the harbor from 09–15 June 1998. Solid line is the seafloor, interpolated between stations. Numbers represent individual and, when available, average concentration measurements. Dashed lines are hand-drawn lines of constant concentration with units = dpm L⁻¹.

irrigation or other mechanisms enhance the radon flux from sediments.

The mixing model

A multibox mixing model was developed to describe water exchange in Catalina Harbor (Fig. 4). The choice of box dimensions was based on the harbor geometry. Box boundaries are shorelines and demarcations shown on Fig. 1, and dimensions were determined from navigation charts (Table 5). All boxes have some area in contact with the sediments.

For each box, a steady-state mass balance equation for radon was written:

$$J_{\text{Prod}} + J_{\text{Benth}} + J_{\text{TP}} = J_{\text{Decay}} + J_{\text{Atm}} + J_{\text{HM}} + J_{\text{Ad}} \quad (4)$$

The terms on the left-hand side of the equation are inputs. The in situ production flux is the product of the ²²⁶Ra activity and the volume of the box: $J_{\text{Prod}} = V_{ij}P$. The radon production rate was defined as 1.66 ± 0.17 atoms s⁻¹ m⁻³, on the basis of measurements made in the San Pedro Channel. The average benthic flux as calculated from the flux chamber measurements (Table 3) is multiplied by the sediment area to compute the flux from the sediments: $J_{\text{Benth}} = J_{\text{sed}}A_{\text{sed}}$. This benthic input included molecular diffusion, irrigation, and possibly other mechanisms captured during the flux chamber deployments. Filling and draining the beach on a tidal cycle, tidal pumping (J_{TP}), was identified as an additional source of radon (see next section) and independently verified in a separate study (Colbert et al. 2008). Submarine groundwater discharge of fresh, meteoric water was initially discounted because of a lack of rainfall and the small size of the watershed. The lack of consistent seepage meter data also supports that fresh groundwater discharge is small. Further, no freshwater was found in the beach at the head of the harbor (Colbert et al. 2008).

On the right-hand side of Eq. 4, the first two fluxes are loss terms for radon. Radioactive decay is equal to the radon activity in a box: $J_{\text{Decay}} = V_{ij}C_{ij}$. Radon gas exchange is characterized by the contrast between surface water ($j = 1$) radon concentrations and that calculated for water in equilibrium with a gas phase:

$$J_{\text{Atm}} = \frac{kA_{\text{surf},i1}(\lambda C_{i1} - \lambda C_a)}{\lambda} \quad (5)$$

The atmospheric concentration λC_a was measured (69 ± 4 dpm m⁻³) and the rate of gas exchange was defined as a piston velocity, k . During this study, a piston velocity of 1.5 m d⁻¹ was measured 10 km east of Catalina Harbor, near the center of San Pedro Channel (unpubl. data). However, Catalina Harbor is sheltered by surrounding topography, and we estimated that at the lower wind speeds and fetches, the piston velocity might be approximately 0.5 ± 0.2 m d⁻¹, on the basis of a compilation of Clark and coworkers (1994).

The last two terms on the right-hand side of Eq. 4 are for horizontal mixing (J_{HM}) and advective transport (J_{Ad}). A schematic drawing of the mixing between boxes is shown in

Table 3. Benthic flux measurements made at two stations. Positive fluxes are out of sediment, negative fluxes are into sediment. Jazz has open tube to bottom water, Rock and Blues are sealed.

Sta. ID	Chamber ID	Date deployed	Deployment time (h)	Radon flux (atoms m ⁻² s ⁻¹)	Oxygen flux (mmol m ⁻² day ⁻¹)
Near B	Jazz	11 Jun 98	22	35±8	
Near B	Blues	11 Jun 98	22	66±18	-12
Near B*	Rock	11 Jun 98	22	(34±11)	(-14)
Near B	Jazz	12 Jun 98	25	78±13	-12
Near A	Jazz	15 Jun 98	20	96±8	-9
Mean±SE				69±13	-11

*Chamber Rock was excluded from mean because initial radon measurement suggested disturbance.

Fig. 4. Horizontal exchange between boxes was characterized as diffusive:

$$J_{HM,ij} = \frac{K_h A_{ij-i-1,j}}{\lambda X_{ij-i-1,j}} (\lambda C_{i-1,j} - \lambda C_{ij}) + \frac{K_h A_{ij-i+1,j}}{\lambda X_{ij-i+1,j}} (\lambda C_{i+1,j} - \lambda C_{ij}) \quad (6)$$

where A is the contact area between boxes demarcated by subscripts ij , X is the separation of box midpoints, and K_h is the horizontal eddy diffusivity. To assess the average mixing rates, horizontal diffusivity was assumed identical between all boxes.

On the basis of the temperature profiles, upwelling appears to occur near the head of the harbor. Upwelling was simulated in the model as an advection of water, and was assumed to dominate over vertical diffusion. The advective flux out of a box is defined as:

$$J_{Ad,ij} = -Q_{ij-i'j'} C_{ij} \quad (7)$$

where $Q_{ij-i'j'}$ (m³ s⁻¹) is the advective flux of water from box ij into box $i'j'$. The input flux to the adjacent box is $-J_{Ad,ij}$. To conserve mass, the advective flux of water upwelled must be balanced by an onshore flow of water at depth and an offshore flow of water at the surface (Fig. 4):

$$Q_{42-32} + Q_{33-32} = Q_{32-22} + Q_{32-31} = Q_{31-41} \quad (8)$$

By this formulation, all of the water that upwells passes through box 32 and box 31.

Table 4. Radon emanation rate and calculated radon production rate in a sediment core collected at Sta. B. Radon emanation rate uncertainty is 1 SD on the basis of counting statistics. Radon production rate uncertainty is calculated by the propagation of errors.

Sediment depth (cm)	Porosity	Emanation rate (E) (dpm g ⁻¹)	Radon production rate (P) (dpm L ⁻¹)
0–3 cm	0.66±0.01	0.119±0.003	160±7
3–6 cm	0.53±0.01	0.076±0.002	180±7
6–9 cm	0.47±0.01	0.067±0.003	200±9
11–13.5 cm	0.40±0.01	0.069±0.002	270±11

Tidal pumping—The magnitude of the radon inputs and outputs was assessed by examining the mass balance for the head of the harbor (box 11). An estimate of the mixing can be made on the basis of the average flow of the tidal prism:

$$Q_{11-21} = \frac{H A_{Surf,11}}{\tau} = K_h \frac{A_{11-21}}{X_{11-21}} \quad (9)$$

where H is the average tidal range (1.1 m), $A_{Surf,ij}$ is the box upper surface area, and τ is the tidal period. For box 11, the maximum tidal exchange flux is 0.9 m³ s⁻¹. When this value is used to calculate the mass balance for the head of the harbor, an additional source of radon is required. Simplifying Eq. 4, since there is no vertical mixing and horizontal mixing with only one box, the additional flux is:

$$J_{TP,11} = J_{Decay,11} + J_{Atm,11} + Q_{11-21} (\lambda C_{21} - \lambda C_{11}) - J_{Prod,11} + J_{Benth,11} \quad (10)$$

where the radon fluxes required to compute these terms were presented above. With this formulation, the additional flux into box 11 is about 7×10^6 atom s⁻¹. This additional radon was presumably from tidal pumping (J_{TP}),

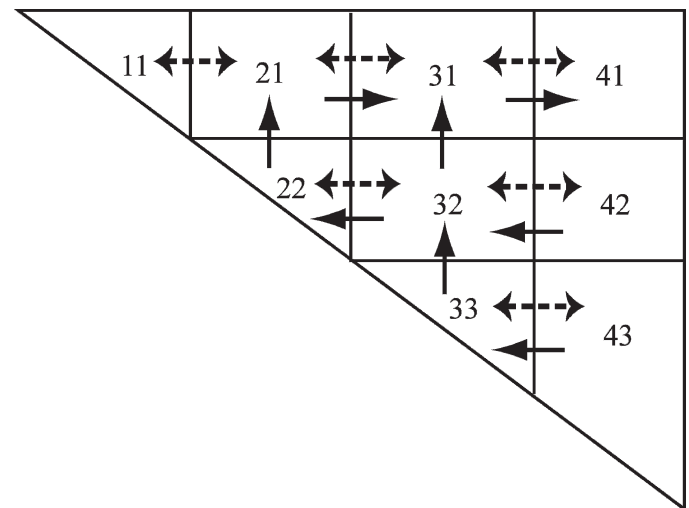


Fig. 4. Box model schematic showing box numbering and arrows to indicate horizontal eddy diffusion (two-headed dashed arrows) and advection (solid arrows). All boxes have some contact with sediment. Surface boxes exchange with the atmosphere and receive input from tidal pumping. Box dimensions are detailed in Table 5.

Table 5. Physical characteristics of each box used in the mixing model.

Box	Stations (<i>n</i> analysis)	Avg. Rn conc. (dpm m ⁻³)	Volume (10 ⁴ m ³)	Upper area (10 ⁴ m ²)	Sed. area (10 ⁴ m ²)	Shoreline (m)	Seaward area (m ²)	Separation (m)	Avg. thickness (m)
11	A (2)	1,780	6.60	5.09	5.09	826	247	372	1.3
21	B,BC,C (4)	1,100	17.6	9.09	5.10	855	271	395	1.9
22	B,BC,C (4)	500	11.9	3.99	3.99		584	395	3.0
31	D,E (4)	510	31.6	16.6	2.44	1,092	684	484	1.9
32	E (3)	320	55.7	14.2	7.38		1,156	484	3.9
33	E (1)	380	34.0	6.81	6.81		1,805	484	5.0
41	F (2)	120							
42	F (1)	120							
43	F (2)	170							

the circulation of water through beach sediments with the rise and fall of the tides. The tidal pumping flux into each surface box was the product of the length of shoreline and the normalized input flux calculated for box 11, $J_{TP,ij} = J_{SL}L_{ij}$. For the model, mixing out of box 11, and thus the tidal pumping flux, was left as an independent variable. A comparison between the model-derived mixing rate and the tidal mixing rate is discussed in the next section.

Model results—The model was fit to the observed radon distribution by tuning four independent variables: K_h , Q_{31-41} , Q_{32-31} , and Q_{42-32} . The best fit of the model to the data was computed by minimizing the following function:

$$\psi = \sqrt{\sum \left(\frac{\sum F_{ij}}{\sum F_{out,ij}} \right)^2} \quad (11)$$

where the numerator is the sum of all the fluxes for box *ij* and the denominator is the sum of only the losses (losses by mixing and advection, radioactive decay, and evasion). For the total model, inputs and outputs were balanced to within 0.02%, well within the uncertainty of the individual measurements (Table 6). The best fit to the model was with a horizontal mixing rate of 0.54 ± 0.19 m² s⁻¹ and an upwelling flux of water was 1.5 ± 0.7 m³ s⁻¹. The model sensitivity to the mixing rate and the total flux of water upwelled was assessed by varying these values and calculating the cost function ψ . For this analysis, the fractions of water upwelled into and out of box 31 (Q_{42-32} and Q_{32-31}) were held constant. The uncertainty on K_h and

Q_{31-41} was assigned assuming that a doubling of the cost function ψ was equivalent to 1 SD. The model was not very sensitive to the upwelling flux, with the cost function increasing slowly beyond 1 SD. The model was more sensitive to the mixing rate. At low values of K_h , the cost function increased rapidly. At higher values of K_h , the cost function steadily increased.

The model-derived J_{TP} was $5,200 \pm 1,900$ atoms s⁻¹ (m shoreline)⁻¹. This estimate is consistent with direct measurements of the J_{TP} ($4,000 \pm 1,500$ atom s⁻¹ [m shoreline]⁻¹) made during a later study at Catalina Harbor (Colbert et al. 2008). The agreement of mass balance estimate of J_{TP} with observations gives us greater confidence that the mixing rate and piston velocity are correct. This also suggests that other sources of radon, including sediment resuspension, physical pumping of water through sediments by currents interacting with seafloor topography, and fresh groundwater inputs, were negligible. For surface boxes, tidal pumping accounts for more than 50% of the radon input (Table 6). Benthic inputs were the other primary source of radon. In situ production was only a minor component. For box 11, about half the radon was lost by evasion to the atmosphere, and the remaining half was divided equally between mixing and radioactive decay.

The best fit to the model was with a mixing rate of 0.54 ± 0.19 m² s⁻¹. Using Eq. 9, the horizontal exchange rate (Q_{ij}) was calculated from K_h . Horizontal exchange increased offshore as the surface area between boxes increased, from 0.4 m³ s⁻¹ between boxes 11 and 21 to 2.0 m³ s⁻¹ between boxes 33 and 43. For box 11, the tidal exchange flux (0.9 m³ s⁻¹) was more than twice the

Table 6. The mixing model. Radon fluxes and mass balance for each box in units of 106 atoms s⁻¹. Negative fluxes are sinks, positive fluxes are sources. The last column is the sum of the sources and sinks for each box.

Box	Inputs					Outputs				Box sum
	In situ production	Benthic input	Tidal pumping	Horizontal mixing	Advection	Decay	Evasion	Horizontal mixing	Advection	
11	0.11	3.51	4.36			-1.96	-4.00	-2.02		0.00
21	0.29	3.52	4.52	2.02	1.42	-3.23	-4.31	-1.82	-3.13	-0.70
22	0.20	2.75			0.91	-0.99		-1.19	-1.42	0.25
31	0.53	1.68	5.77	1.82	6.05	-2.69	-3.37	-2.47	-6.12	1.21
32	0.93	5.09		1.19	1.44	-2.97		-2.14	-3.84	-0.30
33	0.57	4.70			0.00	-2.15		-3.51	0.00	-0.40
Totals	2.62	21.26	14.65	5.03	9.82	-13.98	-11.68	-13.16	-14.50	0.06

exchange on the basis of the K_h estimate, suggesting that a significant fraction of the water that flushes out of box 11 on the ebb tide was returned on the flood tide. The mixing rate can also be compared with Okubo's (1976) empirical relationship between K_h and scale. For length scales of 200 m (harbor width) to 450 m (station spacing), K_h should fall in the range of 0.6 to 1.5 m² s⁻¹. Given the uncertainty in the measurement, it appears that eddy diffusion in this system can be accurately characterized by its length scale.

The model-derived upwelling flux of water was 1.5 ± 0.7 m³ s⁻¹. This generated a seaward horizontal advection of about 200 m d⁻¹ out of box 31. About 21% of the water upwelled into box 21, and the rest upwelled into box 31. The upwelling velocities into box 21 and box 31 (the flux divided by the box surface area) were remarkably similar and averaged 0.73 m d⁻¹. This suggests that similar results would have been derived if the model was formulated with only three independent variables: K_h , the upwelling velocity, and the upwelling flux into box 32. At this rate, box 21 was flushed with upwelling seawater every 5.6 d, and box 31 was flushed every 3 d. Including advection from box 21, the flushing time for box 31 is further reduced. From a management point of view, potential sources of pollution should be placed in box 31, where they will be flushed out of the harbor relatively quickly. Pollutants that enter into box 21 will be retained in the harbor for a longer period and have a better chance of mixing toward the beach at the head of the harbor.

The model predicted that there was no upwelling between box 33 and box 32, which violates the assumption that vertical mixing is negligible. The model also predicted that there was no onshore flow at the bottom of the water column from box 43 to box 33. But the temperature profiles suggest an onshore flow of cold, deep water near the seafloor that extends past Sta. C. These differences between the model and observations suggest that the single measurement used to characterize the concentration in box 33 was not representative of the average concentration. A lower concentration in box 33 would have been consistent with an onshore advection of deep seawater at depth and upwelling into box 32.

To summarize, two primary sources of radon were identified in Catalina Harbor. First, benthic inputs were measured and found to be enhanced relative to molecular diffusion by irrigation. Second, on the basis of a mass balance for radon, tidal pumping of water through shoreline sediments was also identified as an important source. At the head of Catalina Harbor, tidal pumping accounted for 54% of the total input of radon. The mass balance was also used to constrain the radon losses. Boxes at the surface lost a significant amount of radon to the atmosphere, but for other boxes that have a greater mean depth or are isolated from the atmosphere, decay was much more important. Upwelling was identified on the basis of the thermal structure, and model-derived upwelling rates were 0.73 m d⁻¹ across most of the harbor. The exchange coefficients defined by the radon simulation are consistent with those predicted on the basis of scaling arguments and can now be used to estimate mixing and transport of nutrients and contaminants in Catalina Harbor.

References

- BERELSON, W. M. 1986. Studies of water column mixing and benthic exchange of nutrients, carbon, and radon in the Southern California Borderland. Ph.D. Thesis, Univ. of Southern California.
- , D. E. HAMMOND, AND A. EATON. 1987. A technique for the rapid extraction of Rn-222 from water samples and a case study, p. 271–281. *In* B. Graves [ed.], Radon in groundwater. National Water Well Association.
- , ———, AND C. FULLER. 1982. Radon-222 as a tracer for mixing in the water column and benthic exchange in the southern California borderland. *Earth Planet. Sci. Lett.* **61**: 41–54.
- BROECKER, W. S. 1965. The application of natural radon to problems in ocean circulation, p. 116–145. *In* T. Ichiye [ed.], Symposium on diffusion in oceans and fresh waters. Lamont-Doherty Geological Observatory.
- , L. J. CROMQWELL, AND Y.-H. LI. 1968. Rates of vertical eddy diffusion near the ocean floor based on measurements of the distribution of excess ²²²Rn. *Earth Planet. Res. Lett.* **5**: 101–105.
- , AND T.-H. PENG. 1971. Vertical distribution of radon in BOMEX area. *Earth Planet. Res. Lett.* **11**: 99–109.
- CABLE, J. E., W. BURNETT, J. CHANTON, AND G. WEATHERLY. 1996. Estimating groundwater discharge into the northeastern Gulf of Mexico using radon-222. *Earth Planet. Res. Lett.* **144**: 591–604.
- CLARK, J. F., R. WANNINKHOF, P. SCHLOSSER, AND H. J. SIMPSON. 1994. Gas exchange rates in the tidal Hudson River using a dual tracer technique. *Tellus B* **46**: 274–285.
- COLBERT, S. L., W. M. BERELSON, AND D. E. HAMMOND. 2008. Radon-222 budget in Catalina Harbor, California: 2. Flow dynamics and residence time in a tidal beach. *Limnol. Oceanogr.* **53**: 659–665.
- HAMMOND, D. E., AND C. FULLER. 1979. The use of radon-222 to estimate benthic exchange and atmospheric exchange rates in San Francisco Bay, p. 213–230. *In* T. J. Conomos [ed.], San Francisco Bay: The urbanized estuary. Pacific Div. Amer. Assoc. Adv. Sci.
- JÄHNE, B., G. HEINZ, AND W. DIETRICH. 1987. Measurement of the diffusion coefficients of sparingly soluble gases in water. *J. Geophys. Res.* **92**: 10767–10776.
- KEY, R. M., R. L. BREWER, J. H. STOCKWELL, J. GUINASSO, N. L., AND D. R. SCHINK. 1979. Some improved techniques for measuring radon and radium in marine sediments and seawater. *Mar. Chem.* **7**: 251–264.
- MATHIEU, G. G., P. E. BISCAYE, R. A. LUPTON, AND D. E. HAMMOND. 1988. System for measurement of ²²²Rn at low levels in natural waters. *Health Phys.* **55**: 989–992.
- OKUBO, A. 1976. Remarks on the use of 'diffusion diagrams' in modeling scale dependent diffusion. *Deep Sea Res.* **23**: 1213–1214.
- SMETHIE, W. M., JR., C. A. NITROUER, AND R. F. L. SELF. 1981. The use of radon-222 as a tracer of sediment irrigation and mixing on the Washington continental shelf. *Mar. Geol.* **42**: 173–200.
- , T. TAKAHASHI, AND D. W. CHIPMAN. 1985. Gas exchange and CO₂ flux in the tropical Atlantic Ocean determined from Rn-222 and pCO₂ measurements. *J. Geophys. Res.* **C90**: 7005–7022.
- ULLMAN, W. J., AND R. C. ALLER. 1982. Diffusion coefficients in nearshore marine sediments. *Limnol. Oceanogr.* **27**: 552–556.

Received: 27 April 2007
Accepted: 30 October 2007
Amended: 4 December 2007